Calculation of optical matrix elements in carbon nanotubes

S. V. Goupalov,[1,2] A. Zarifi,[3] and T. G. Pedersen[4]
[1]*Department of Physics, Jackson State University, Jackson, Mississippi 39217, USA*
[2]*A.F. Ioffe Physico-Technical Institute, 26 Polytechnicheskaya, 194021 St. Petersburg, Russia*
[3]*Department of Physics, Yasouj University, Yasouj, Iran*
[4]*Department of Physics and Nanotechnology, Aalborg University, Aalborg, Denmark*
(Received 23 December 2009; revised manuscript received 5 February 2010; published 2 April 2010)

Analytical expressions for dipole matrix elements describing interband optical transitions in carbon nanotubes are obtained for arbitrary light polarization and nanotube chiralities. The effect of the symmetry with respect to the time reversal on the dependences of the optical matrix elements on the quantum numbers of electronic states in carbon nanotubes is studied.

DOI: 10.1103/PhysRevB.81.153402 PACS number(s): 78.67.Ch, 78.30.Na, 78.40.Ri

The dependences of matrix elements for optical transitions in carbon nanotubes on quantum numbers of the electronic states and on the nanotube chiral indices are essential for both the study of the fundamental optical phenomena in carbon nanotubes and the application of optical methods for their characterization. Two different approaches have been used to calculate the dipole optical matrix elements within the tight-binding method. The first approach proposed by Jiang *et al.*[1] is based on the introduction of the so-called atomic dipole vectors. Jiang *et al.* derived an analytical expression for the optical matrix element for the case of the parallel polarization valid for all allowed optical transitions between various subbands of the valence and conduction bands of carbon nanotubes. They also tried to extend their treatment to transitions excited by light polarized perpendicular to the nanotube cylindrical axis in armchair nanotubes. However, as it was recently pointed out[2] and is discussed below, this attempt was not quite correct. The method of Jiang *et al.* was further developed in Ref. 2 resulting in the calculation of the optical matrix elements for perpendicular polarization. However, the derivation of Ref. 2 was quite laborious while the final result was obtained in a rather complicated form.

An alternative method was proposed in Ref. 3. There it was applied to calculate matrix elements of optical transitions within the effective-mass scheme accounting for a few lowest (uppermost) subbands of the conduction (valence) band of a carbon nanotube. In the present paper we show that extension of this method to account for all possible interband transitions yields an elegant and straightforward derivation of the optical matrix elements for arbitrary polarizations and nanotube chiralities. We obtain an original analytical expression for the case of the perpendicular polarization. We then compare two different schemes accounting for the electron states in carbon nanotubes and get further insight into their optical properties.

The findings of Ref. 3 can be summarized as follows. Calculation of optical matrix elements in carbon nanotubes within the nearest-neighbor tight-binding method can be divided into two tasks: (1) calculation of the $\mathbf{k}$ dependences of the column coefficients $\hat{C}(s,\mathbf{k})$ of the tight-binding method, and (2) expression of the optical matrix elements in terms of these coefficients. While for the first task the *graphene band structure and zone folding* are essential, it is the nanotube's *cylindrical geometry* which is relevant for an accomplishment of the second task.

In Ref. 3 the first task was performed using the effective-mass scheme and the results were formulated in terms of $\mathbf{\Delta k}$ counted out from the $\mathbf{K}$ or $\mathbf{K}'$ points of the graphene's Brillouin zone. However, the derivation used to accomplish the second task is insensitive to the choice of the origin in the $\mathbf{k}$ space and remains valid when a more traditional zone-folding scheme[4] is applied to find the coefficients $\hat{C}(s,\mathbf{k})$.

For example, the interband *coordinate* matrix element for *parallel* polarization was found in Ref. 3 in the form (we use the notations of Refs. 1, 2, and 4)

$$\langle v,\mathbf{k}'|z|c,\mathbf{k}\rangle = i\delta_{\mu,\mu'}\delta_{K_2,K_2'}\sum_{b=A,B} C_b^*(v,\mathbf{k}')\frac{\partial C_b(c,\mathbf{k})}{\partial K_2}. \quad (1)$$

Here $\mathbf{k}$ refers to the electron two-dimensional wave vector in graphene and has the components K_1 along the nanotube's circumference and K_2 along the nanotube's cylindrical axis. In a nanotube the wave vector K_1 becomes quantized: $K_1^\mu = \mu/R$, where R is the nanotube's radius. The key idea in deriving Eq. (1) [and its counterpart for the perpendicular polarization, Eq. (7)] was to use the fact that the periodic in z Bloch functions belonging to the same K_2 but different band indices s ($s=c,v$) and μ_s form a complete set of functions.

Within the zone-folding scheme the coefficients $\hat{C}(c,\mathbf{k})$ and $\hat{C}(v,\mathbf{k})$ are found to be[1,2,4]

$$\hat{C}(c,\mathbf{k}) \equiv \begin{pmatrix} C_A(c,\mathbf{k}) \\ C_B(c,\mathbf{k}) \end{pmatrix} = \frac{1}{\sqrt{2}}\begin{pmatrix} e^{i\varphi_c} \\ 1 \end{pmatrix}, \quad \hat{C}(v,\mathbf{k}) \equiv \begin{pmatrix} C_A(v,\mathbf{k}) \\ C_B(v,\mathbf{k}) \end{pmatrix} = \frac{1}{\sqrt{2}}\begin{pmatrix} -e^{i\varphi_v} \\ 1 \end{pmatrix}, \quad (2)$$

where

$$\varphi_{c,v} = \begin{cases} \arctan\dfrac{\mathcal{B}}{\mathcal{A}} & \mathcal{A}>0 \\ \arctan\dfrac{\mathcal{B}}{\mathcal{A}}+\pi & \mathcal{A}<0, \end{cases}$$

$$\mathcal{A} = 2\cos(k_x a/2\sqrt{3})\cos(k_y a/2) + \cos(k_x a/\sqrt{3}),$$

$$\mathcal{B} = 2\sin(k_x a/2\sqrt{3})\cos(k_y a/2) - \sin(k_x a/\sqrt{3}),$$

$k_x = K_1^\mu \cos\alpha - K_2 \sin\alpha$, $k_y = K_1^\mu \sin\alpha + K_2 \cos\alpha$ (in the notations of Ref. 3 $k_x \to k_x'$, $k_y \to k_y'$, $K_1 \to k_x$, and $K_2 \to k_y$), a is the lattice constant of graphene, and the angle α is related to the nanotube chiral angle θ by $\alpha = \pi/6 - \theta$. Then Eq. (1) yields

$$\langle v,\mathbf{k}'|z|c,\mathbf{k}\rangle = i\delta_{\mu,\mu'}\delta_{K_2,K_2'} C_A^*(v,\mathbf{k}')\frac{\partial C_A(c,\mathbf{k})}{\partial K_2}$$

$$= \frac{1}{2}\delta_{\mu,\mu'}\delta_{K_2,K_2'} e^{i(\varphi_c - \varphi_v')}\frac{\partial \varphi_c}{\partial K_2},$$

where $\varphi_c \equiv \varphi_c(\mathbf{k})$, $\varphi_v' \equiv \varphi_v(\mathbf{k}')$, or

$$|\langle v,\mathbf{k}'|z|c,\mathbf{k}\rangle| = \frac{1}{2}\delta_{\mu,\mu'}\delta_{K_2,K_2'}\left|\frac{\partial \varphi_c}{\partial K_2}\right|. \tag{3}$$

For the *velocity* matrix element we get (see, e.g., Eq. (20) of Ref. 3)

$$|\langle v,\mathbf{k}'|v_z|c,\mathbf{k}\rangle| = \frac{\delta_{\mu,\mu'}\delta_{K_2,K_2'}}{2\hbar}[E_{c,\mu}(K_2) - E_{v,\mu}(K_2)]\left|\frac{\partial \varphi_c}{\partial K_2}\right| \tag{4}$$

or

$$|\langle v,\mathbf{k}'|v_z|c,\mathbf{k}\rangle| = \frac{\gamma_0}{\hbar}\delta_{\mu,\mu'}\delta_{K_2,K_2'}\sqrt{1 + 4\cos^2(k_y a/2) + 4\cos(k_y a/2)\cos(\sqrt{3}k_x a/2)}\left|\frac{\partial \varphi_c}{\partial K_2}\right|, \tag{5}$$

where γ_0 is the transfer integral of the tight-binding method.[3,4]

Taking the derivative we get

$$\frac{\partial \varphi_c}{\partial K_2} = \frac{a}{\sqrt{3}}\frac{\sin\alpha[\cos(k_y a/2)\cos(\sqrt{3}k_x a/2) - \cos(k_y a)] - \sqrt{3}\cos\alpha\sin(k_y a/2)\sin(\sqrt{3}k_x a/2)}{1 + 4\cos^2(k_y a/2) + 4\cos(k_y a/2)\cos(\sqrt{3}k_x a/2)}. \tag{6}$$

If this expression is substituted into Eq. (5), one obtains Eq. (11) of Ref. 1.

Now let us turn to the *perpendicular* polarization. The expression for the y component of the *coordinate* matrix element immediately follows from Eqs. (19) and (24) of Ref. 3,

$$\langle v,\mathbf{k}'|y|c,\mathbf{k}\rangle = iR\frac{\delta_{\mu',\mu-1} - \delta_{\mu',\mu+1}}{2}\delta_{K_2,K_2'} \times \sum_{b=A,B} C_b^*(v,\mathbf{k}')C_b(c,\mathbf{k}). \tag{7}$$

Substituting Eq. (2) into Eq. (7) we obtain

$$\langle v,\mathbf{k}'|y|c,\mathbf{k}\rangle = R\delta_{K_2,K_2'}\frac{\delta_{\mu',\mu+1} - \delta_{\mu',\mu-1}}{2}e^{i(\varphi_c - \varphi_v')/2} \times \sin[(\varphi_v' - \varphi_c)/2] \tag{8}$$

or

$$|\langle v,\mathbf{k}'|y|c,\mathbf{k}\rangle| = R\delta_{K_2,K_2'}\left|\frac{\delta_{\mu',\mu+1} - \delta_{\mu',\mu-1}}{2}\right||\sin[(\varphi_v' - \varphi_c)/2]|. \tag{9}$$

For the *velocity* matrix element we get from this [see, e.g., Eq. (20) of Ref. 3]

$$|\langle v,\mathbf{k}'|v_y|c,\mathbf{k}\rangle| = \frac{R}{\hbar}\delta_{K_2,K_2'}[E_{c,\mu}(K_2) - E_{v,\mu'}(K_2)] \times \left|\frac{\delta_{\mu',\mu+1} - \delta_{\mu',\mu-1}}{2}\right||\sin[(\varphi_v' - \varphi_c)/2]|. \tag{10}$$

Equations (9) and (10) are original and constitute the main result of the present paper.

In Figs. 1–4 matrix elements of the velocity operator for interband transitions in a (4,2) carbon nanotube calculated using Eq. (10) are shown (for the sake of brevity, we use the notation $|v_y| \equiv |\langle v,\mu,K_2|v_y|c,\mu+1,K_2\rangle|$; T is the length of the nanotube's translational vector[4]). If the incident light has a circular polarization causing the transitions of the type $v,\mu \to c,\mu+1$ then Figs. 1–4 exhaust all the possible *interband* transitions.

Note that the (4,2) nanotube has a small radius and, therefore, the effective-mass scheme does not work well for this nanotube.[5] However, it can still be applied to a couple of lowest conduction or uppermost valence bands. For these bands, apart from the $\mu' \to \mu$ labels for optical transitions within the zone-folding scheme, the alternative transition nomenclature is also shown in brackets in Figs. 2 and 3. The correspondence between the two nomenclatures is most easily seen on a plot where a line segment representing the

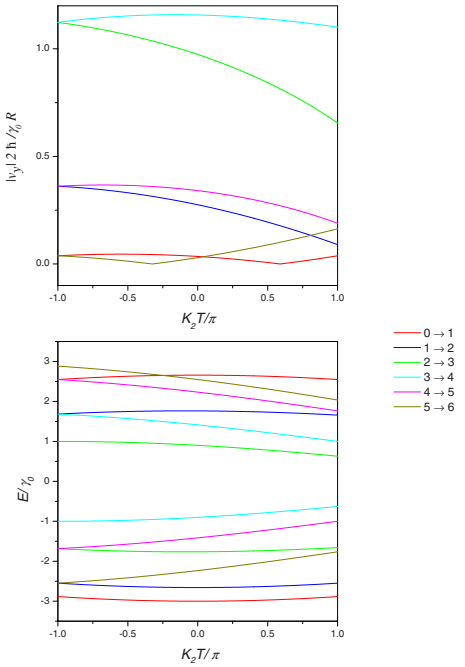

FIG. 1. (Color online) Velocity matrix elements (upper panel) and energy bands (lower panel) for some interband optical transitions in a (4,2) carbon nanotube. Incident light is polarized perpendicular to the nanotube axis, z.

nanotube's Brillouin zone is shown for each K_1^μ in the reciprocal space of graphene (see Fig. 5). For a (4,2) nanotube the line segment corresponding to $\mu=9$ is the most close line segment with respect to any of the $\mathbf{K}$ points in the reciprocal space of graphene. Similarly, the line segment corresponding to $\mu=19$ is the most close line segment with respect to any of the $\mathbf{K}'$ points.

The states $\mathbf{K},n,K_2$ and $\mathbf{K}',-n,-K_2$ in the nomenclature of the effective-mass scheme are related to one another by

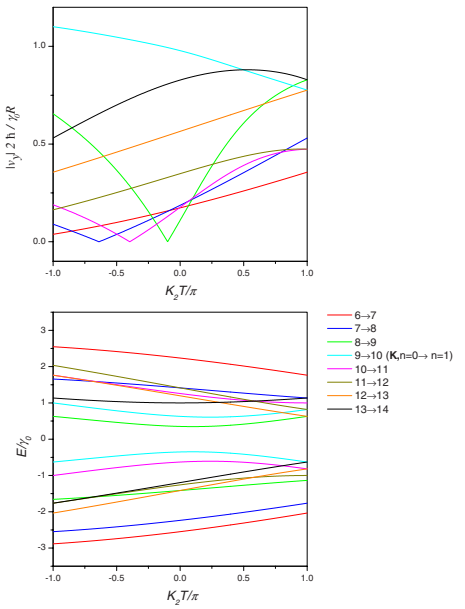

FIG. 2. (Color online) Same as Fig. 1 except for subband indices.

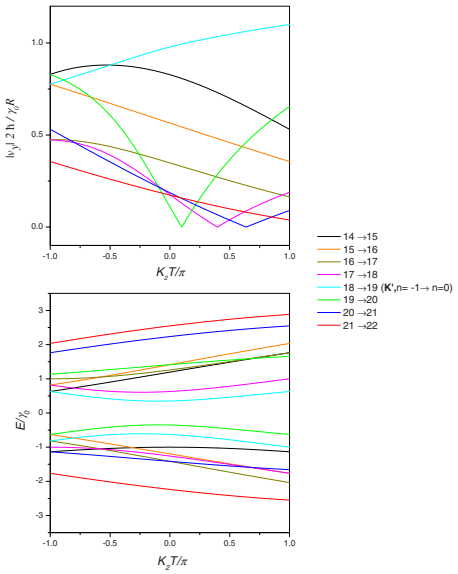

FIG. 3. (Color online) Same as Fig. 1 except for subband indices.

the time inversion symmetry.[6] (Strictly speaking, within the effective-mass scheme one should characterize the states in the $\mathbf{K}$ and $\mathbf{K}'$ valleys by ΔK_2 and $\Delta K_2'$, respectively, but, as for $\mathbf{K}$ and $\mathbf{K}'$ indicated in Fig. 5 one has $\mathbf{K}\mathbf{K}_2=-\mathbf{K}'\mathbf{K}_2$, the sign of Δ can be omitted). At the same time, there is a mirrorlike symmetry between the energies of the conduction- and valence-band electronic states of the nanotube.[7] For these reasons the dependences of the absolute values of the interband matrix elements of v_y for the $9\rightarrow10$ transition in Fig. 2 and for the $18\rightarrow19$ transition in Fig. 3 are related to each other by the reflection with respect to the line $K_2=0$. Similar relations exist between the states $\mu_1=9+n,K_2$ and

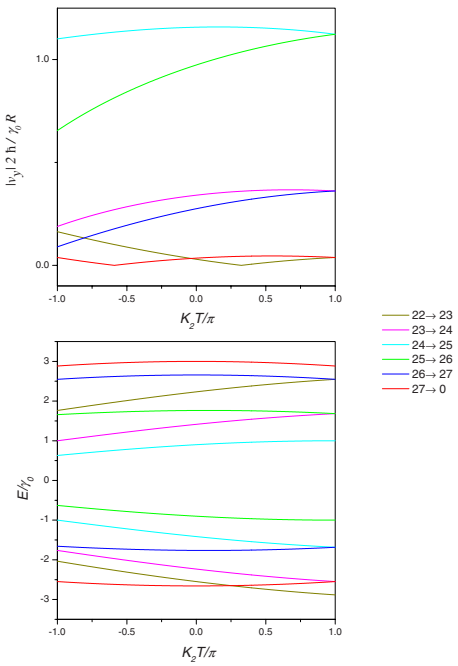

FIG. 4. (Color online) Same as Fig. 1 except for subband indices.

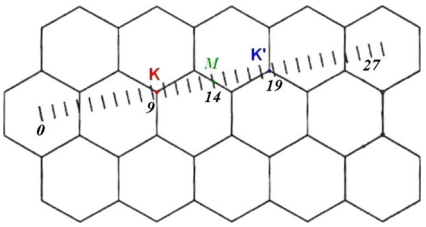

FIG. 5. (Color online) The 29 replicas of the Brillouin zone of a (4,2) carbon nanotube (corresponding to the 28 subbands in the conduction or valence band) superimposed upon the reciprocal lattice of graphene. The 0th and the 28th replicas correspond to the same subband. See Fig. 3.5 of Ref. 4 for more details.

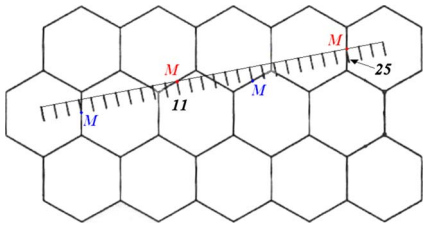

FIG. 6. (Color online) Illustration of an additional symmetry peculiar for the (4,2) nanotube.

$\mu_2=19-n,-K_2$ and, therefore, between the transitions $v,\mu'=9+n\rightarrow c,\mu=10+n$ and $v,\mu'=18-n\rightarrow c,\mu=19-n$. For this reason the transitions presented in Fig. 2 and their counterparts in Fig. 3 are shown by the same color. The same relation is held between the transitions shown in Figs. 1 and 4. In a general case of an arbitrary nanotube these pairs of transitions can be represented as $v,\mu'=N/2+l\rightarrow c,\mu=N/2+l+1$ and $v,\mu'=N/2-l-1\rightarrow c,\mu=N/2-l$,[8] where N is the number of hexagons in the one-dimensional unit cell of the carbon nanotube[4] and l is an integer modulo $N/2$.

The situation described above for the (4,2) carbon nanotube is typical for all *chiral* nanotubes. For *achiral* nanotubes one has $|v_y(K_2)|=|v_y(-K_2)|$ and, therefore, the two curves $|v_y(K_2)|$, related by the reflection with respect to the line $K_2=0$ and representing two different transitions, will coincide.[9] For a (m,m) armchair nanotube such pairs of interband transitions are $v,\mu'=m+n\rightarrow c,\mu=m+n+1$ and $v,\mu'=m-n-1\rightarrow c,\mu=m-n$. We would like to emphasize that this coincidence is not a consequence of some fundamental symmetry of the physical system under study but merely a property of the model which neglects the overlap integral of the tight-binding method.

It is worth to note that the (4,2) nanotube possesses some extra symmetry peculiar for this particular nanotube. Namely, the states with $\mu=11$, $K_2=\pi/T$; $\mu=25$, $K_2=\pi/T$; $\mu=3$, $K_2=-\pi/T$; and $\mu=17$, $K_2=-\pi/T$ correspond to the **M** points in the reciprocal space of graphene.[10] As illustrated in Fig. 6, this means that the points in the **k** space corresponding to $\mu_1=11-m$, $K_2^{(1)}=\pi/T$ and $\mu_2=11+m$, $K_2^{(2)}=\pi/T$ are symmetric with respect to the **M** point. But we have already seen[8] that such a symmetry is related to the time-reversal operation (all the **M** points are equivalent). Therefore, within our model (neglecting the overlap integral), the values of $|v_y(K_2=\pi/T)|$ coincide for the pairs of transitions $v,\mu'=10-m\rightarrow c,\mu=11-m$ and $v,\mu'=11+m\rightarrow c,\mu=12+m$. The same is true for the pairs of transitions $v,\mu'=24-m\rightarrow c,\mu=25-m$ and $v,\mu'=25+m\rightarrow c,\mu=26+m$, where all the values of μ should be taken modulo 28. Similar relations take place at $K_2=-\pi/T$.

Note that the object of Ref. 3 was to find the dependences of the matrix elements for optical transitions occurring at the points of the van Hove singularities on the radii and chiral angles for various semiconducting nanotubes. To that end it is more convenient to use the expressions for the tight-binding coefficients $\hat{C}(s,\mathbf{k})$ within the effective-mass scheme in the first place (when performing the first task mentioned above) rather than studying particular cases of Eqs. (5) and (10). In this way analytical expressions describing the chirality dependences of the matrix elements for optical transitions occurring at the points of the van Hove singularities were obtained in Ref. 3.

In summary, we have shown that application of the method developed in Ref. 3 yields a simple and straightforward derivation of optical matrix elements for carbon nanotubes. We derived an original analytical expression for the matrix elements governing interband optical transitions polarized perpendicular to the nanotube's cylindrical axis. We studied how the dependences of the optical matrix elements on the quantum numbers of the electronic states are affected by the time-reversal symmetry.

The work of S.V.G. was supported by the NSF under Grant No. HRD-0833178.

[1] J. Jiang, R. Saito, A. Grüneis, G. Dresselhaus, and M. S. Dresselhaus, Carbon **42**, 3169 (2004).
[2] A. Zarifi and T. G. Pedersen, Phys. Rev. B **80**, 195422 (2009).
[3] S. V. Goupalov, Phys. Rev. B **72**, 195403 (2005).
[4] R. Saito, G. Dresselhaus, and M. S. Dresselhaus, *Physical Properties of Carbon Nanotubes* (Imperial College, London, 1998).
[5] In particular, it fails to predict the order of the energy bands.
[6] E. L. Ivchenko and B. Z. Spivak, Phys. Rev. B **66**, 155404 (2002).
[7] As a consequence of the overlap integral of the tight-binding method being neglected. See Ref. 4.
[8] The state with $\mu=N/2,K_2=0$ corresponds to the **M** point in the reciprocal space of graphene. If the origin in the reciprocal space were moved to this point then the time-reversal operation would relate the electronic states of a carbon nanotube characterized by the opposite two-dimensional **k** vectors (the electron spin is neglected). For the (4,2) nanotube $N=28$.
[9] As was pointed out in Ref. 2, this is not the case of Fig. 6 in Ref. 1 describing optical transitions in a (10, 10) armchair nanotube.
[10] For $\mu=11$, $K_2=\pi/T$ one has $\mathbf{K}_1=11(5\mathbf{b}_1+4\mathbf{b}_2)/28$, $\mathbf{K}_2=1/2(2\mathbf{b}_1-4\mathbf{b}_2)/28$, where $\mathbf{b}_1$ and $\mathbf{b}_2$ are the reciprocal-lattice vectors of graphene (Ref. 4). Thus, one has $\mathbf{K}_1+\mathbf{K}_2=2\mathbf{b}_1+3/2\mathbf{b}_2$, which corresponds to the **M** point in the reciprocal space of graphene.